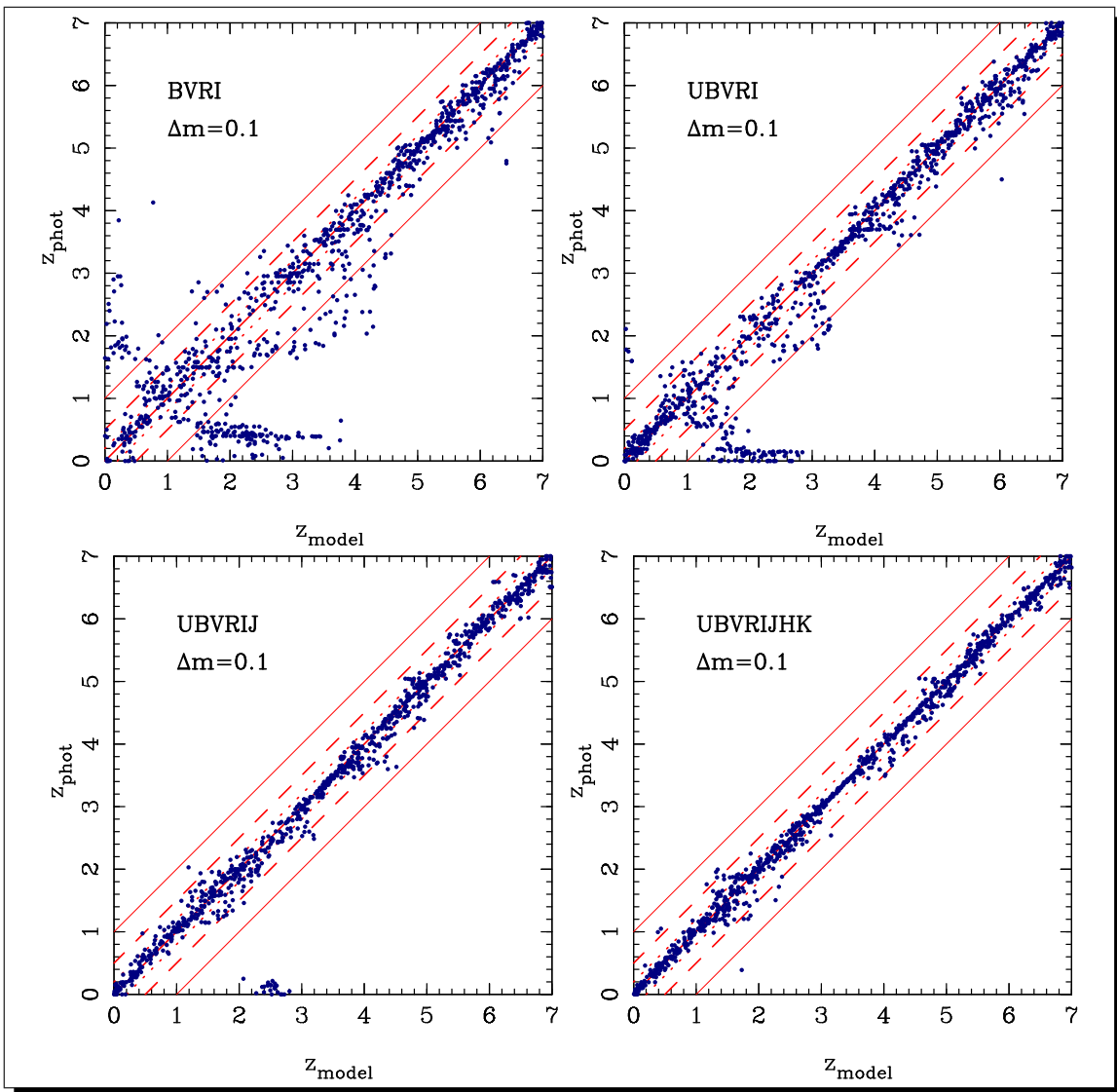


User's manual

Hyperz v1.2

by Micol Bolzonella, Roser Pelló and Joan-Marc Miralles



Contents

1	What are photometric redshifts?	3
1.1	The SED fitting method	3
2	The Hyperz package: overview	4
2.1	Installation	5
2.2	Template SEDs	6
2.2.1	Initial Mass Function	6
2.2.2	Star Formation Rate	9
2.2.3	Metallicity	11
2.3	Reddening	11
2.4	Lyman forest	15
3	Hyperz: Getting started	16
3.1	Procedure	19
3.2	Parameters	20
3.2.1	Inputs	20
3.2.2	Outputs	29
4	Make_catalog: Getting started	30
4.1	Parameters	30
A	Filters and Photometric systems	32
B	FAQ	33
C	Most important changes	35
D	Important remarks	35

1 What are photometric redshifts?

The technique of photometric redshifts can boast a relatively long history. Its first applications date back to the sixties, but recently photometric redshifts have experienced a burst of interest because deep multicolour photometric surveys have been carried out, with a large number of objects inaccessible to spectroscopic observations or too time consuming with the available instruments.

Photometric redshifts are an estimate of the redshift of galaxies (or AGNs, quasars) using only large/medium band photometry instead of spectroscopy. The efficiency of the method relies in the identification of spectral breaks, i.e. strong spectral features, still recognizable after the integration of the Spectral Energy Distribution (hereafter SED) below the filter’s transmission function. The precision of this estimate is worse than the spectroscopic redshift one, depending on the filters set and on the photometric accuracy, but for many cosmological and extragalactic applications the photometric redshift represents a sufficient information. Thus, the photometric redshift tool can be extensively applied and will rapidly become a crucial tool of observational cosmology. This is the reason inducing us to develop a public code, trying to introduce some improvement in the “classical” method, as the inclusion of the redshift probability distributions and of error bars rather than singular values.

Between the two methods most largely used, the empirical training set (e.g. Connolly et al. 1995, Brunner et al. 1997) and the SED fitting (e.g. Lanzetta et al. 1996, Fernández-Soto et al. 1999) we chose the latter, because of its flexibility when different sets of data are used.

1.1 The SED fitting method

The SED fitting procedure to obtain photometric redshifts is based on the fit of the overall shape of the spectra and on the detection of strong spectral properties. To obtain more secure results, the filter set must be chosen in order to bracket some of these features, as the 4000 Å break or the Lyman break at 912 Å. The observed photometric SEDs are compared to those obtained from a set of reference spectra, using the same photometric system. These template SEDs can be either observed or synthetic.

The photometric redshift of a given object corresponds to the best fit of its photometric SED by the set of template spectra, in general through a standard χ^2 minimization procedure. The observed SED of a given galaxy is compared to a set of template spectra:

$$\chi^2(z) = \sum_{i=1}^{N_{\text{filters}}} \left[\frac{F_{\text{obs},i} - b \times F_{\text{temp},i}(z)}{\sigma_i} \right]^2, \quad (1)$$

where $F_{\text{obs},i}$, $F_{\text{temp},i}$ and σ_i are the observed and template fluxes and their uncertainty

in filter i , respectively, and b is a normalization constant.

A combination of this method with the Bayesian marginalization introducing an *a priori* probability was proposed by Benítez (2000): he demonstrated that in this case the dispersion of z_{phot} can be significantly improved. Despite of this result, we decided to not introduce such type of information, because the application of the Bayesian technique can introduce spurious effects in particular studies. However, this method can be regarded with interest when the goal is some specific application or when one is dealing with poor data, in such a way that the introduction of hints allows to obtain useful results. Alternatively, the photometric redshift estimate can be safely improved introducing the Bayesian inference when prior information is not related to the photometric properties of sources. Examples of such priors that could be combined with the z_{phot} technique are the morphology or the clues inferred from gravitational lensing modeling. In these cases, the user can easily introduce the interesting prior in the Fortran 77 code.

The major advantages of the SED fitting technique are its simplicity and the fact that it does not require any spectroscopic sample. Its weak point is mainly related to the need to choose fiducial spectral templates valid for all objects. We will discuss our choice in the following.

2 The Hyperz package: overview

The public package contains the code to obtain photometric redshifts, called **hyperz** and described in Section 3, as well as a program called **make_catalog**, illustrated in Section 4. The second program is useful to build synthetic photometric catalogues and to carry out tests on the attainable accuracy when recovering the redshift given a filter set and a photometric accuracy (see Bolzonella et al. 2000). There is no difference in the use of **hyperz** between observed and simulated catalogues. Here we report the steps to retrieve and install these programs and the ingredients used to build them. The source files and the binary files containing template SEDs (see later) are available on the web at the address

<http://webast.ast.obs-mip.fr/hyperz>

and mirrored at the addresses <http://cosmos.ifctr.mi.cnr.it/micol/> and <http://www.astro.uni-bonn.de/~miralles/hyperz/>. Take care to retrieve the files corresponding to the type of machine you are using: for the source files you have to choose between the IBM version and the default version, working on all other machines. Regarding the binary files, the “big endian” standard works in general under Digital Unix (with the compiler option `-convert big_endian`), SUN, HP, whereas “little en-

dian” binary files have to be downloaded only under Linux system or Digital Unix (without need of compiler options).

2.1 Installation

To extract files, type

```
> gunzip zphot_src_1.2.tar.gz
> tar xvf zphot_src_1.2.tar
> gunzip zphot_big_endian.tar.gz
> tar xvf zphot_big_endian.tar
```

If your machine works with the little endian format for binary files, you have to retrieve the tar file of binary files `zphot_little_endian.tar.gz` instead of the previous one, then

```
> gunzip zphot_little_endian.tar.gz
> tar xvf zphot_little_endian.tar
```

These commands unpack the tar file in a directory named `./ZPHOT/` containing files and subdirectories. Take a look at the `./ZPHOT/src/Makefile` and modify it if needed, according to your compiler and your machine. Now you can compile the Fortran 77 sources typing

```
> cd ./ZPHOT/src
> make hyperz
> make catalog
> make clean
```

In this way you have created the executables **hyperz** and **make_catalog**, that will be automatically copied in the `$HOME/bin` directory (check before “make” and create it if it does not exist). To run the programs from any directory, update your `.login` (`.cshrc`, `.tcshrc` or equivalent) with

```
> source .login
```

after checking the presence of `$HOME/bin` in your login paths.

Both the programs use a parameter file to control input-output data. In the new version the parameter file is named `hyperz.param` and it is the same for **hyperz** and **make_catalog**. For consistency with the previous versions of the code, the old parameter files `zphot.param` and `catalog.param` can also be used without generating errors. The parameters contained in `hyperz.param` will be detailed in Section 3. Here we will describe one basic ingredient, namely the template SEDs provided with the package, and their handling.

2.2 Template SEDs

In the **hyperz** package we provided both observed SEDs and spectral synthesis models, but the set of template SEDs can be changed by the user. The mean spectra of local galaxies from Coleman, Wu & Weedman (1980, hereafter CWW) are the most popular among the observed SEDs. In Figure 1 we show the four CWW template spectra, extended in the UV and IR regions by means of Bruzual & Charlot spectra with parameters (SFR and age) selected to match the observed spectra at $z = 0$. These SEDs are contained in the files

```
./ZPHOT/templates/CWW_E_ext.sed  
./ZPHOT/templates/CWW_Sbc_ext.sed  
./ZPHOT/templates/CWW_Scd_ext.sed  
./ZPHOT/templates/CWW_Im_ext.sed
```

In the panorama of synthetic spectra we chose the GISSEL98 (Galaxy Isochrone Synthesis Spectral Evolution Library) spectral evolution library of Bruzual & Charlot (1993), because of its easy implementation, good accuracy, spectral coverage from UV to far-IR, and possibility of spectral evolution to high redshift.

The stellar population synthesis models are based on stellar tracks libraries; then, a spectral energy distribution is assigned to all stars on the evolutionary tracks. Then, the Initial Mass Function (IMF) and the Star Formation Rate (SFR) must be specified to follow the evolution of the integrated spectrum.

2.2.1 Initial Mass Function

The IMF $\xi(M)$ specifies the distribution in mass of a newly formed stellar population and it is frequently assumed to be a simple power law: $\xi(M) = c M^{-(1+x)}$. In general, $\xi(M)$ is assumed to extend from a lower to an upper cutoff, chosen to be $M_1 = 0.1 M_\odot$ and $M_2 = 125 M_\odot$ in GISSEL. In Table 1 we show the parameters of the three most used IMFs: the Salpeter (1955), Scalo (1986) and Miller & Scalo (1979) laws, in the form used by Bruzual & Charlot in their evolutionary synthesis model.

The different slopes of the three considered laws produce different spectral energy distributions: the Scalo and Miller & Scalo laws are flat at small masses and less rich of massive stars with respect to the Salpeter law, as illustrated in Figure 2. The large number of massive stars in the Salpeter law produces an excess of UV flux, whereas the Scalo law generates too many solar mass stars, making the spectrum too red to match the observed colours.

We adopted the Miller & Scalo law as a good compromise. We also tested the influence of a change in IMF, finding a negligible effect in photometric redshift computation (Bolzonella et al. 2000).

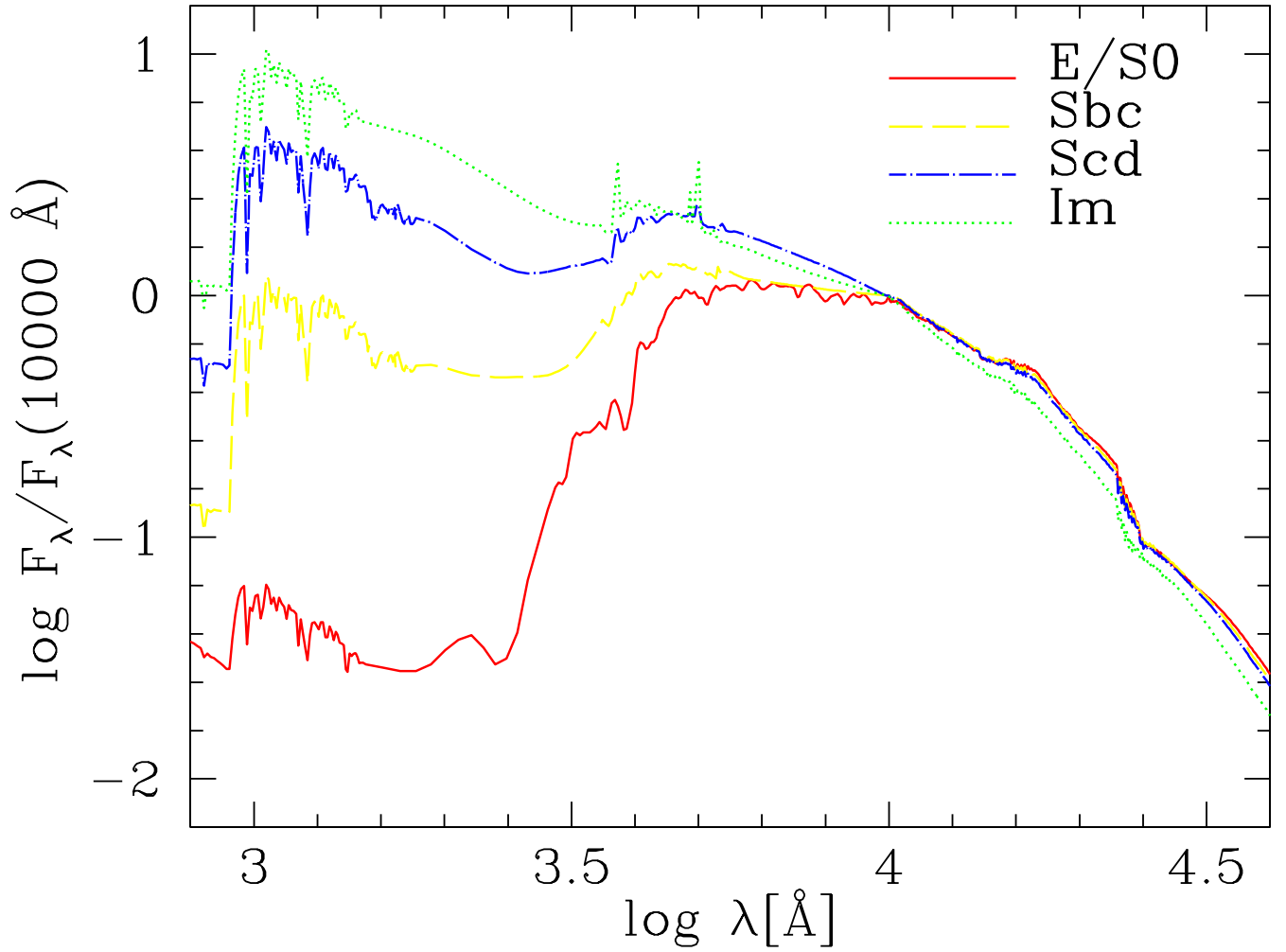


Figure 1: The four CWW mean observed spectra of local galaxies. Because the original data of CWW extend only from 1400 to 10000 \AA , we extrapolate the templates at ultraviolet and near-infrared wavelengths using the spectral evolutionary models of Bruzual & Charlot (1993).

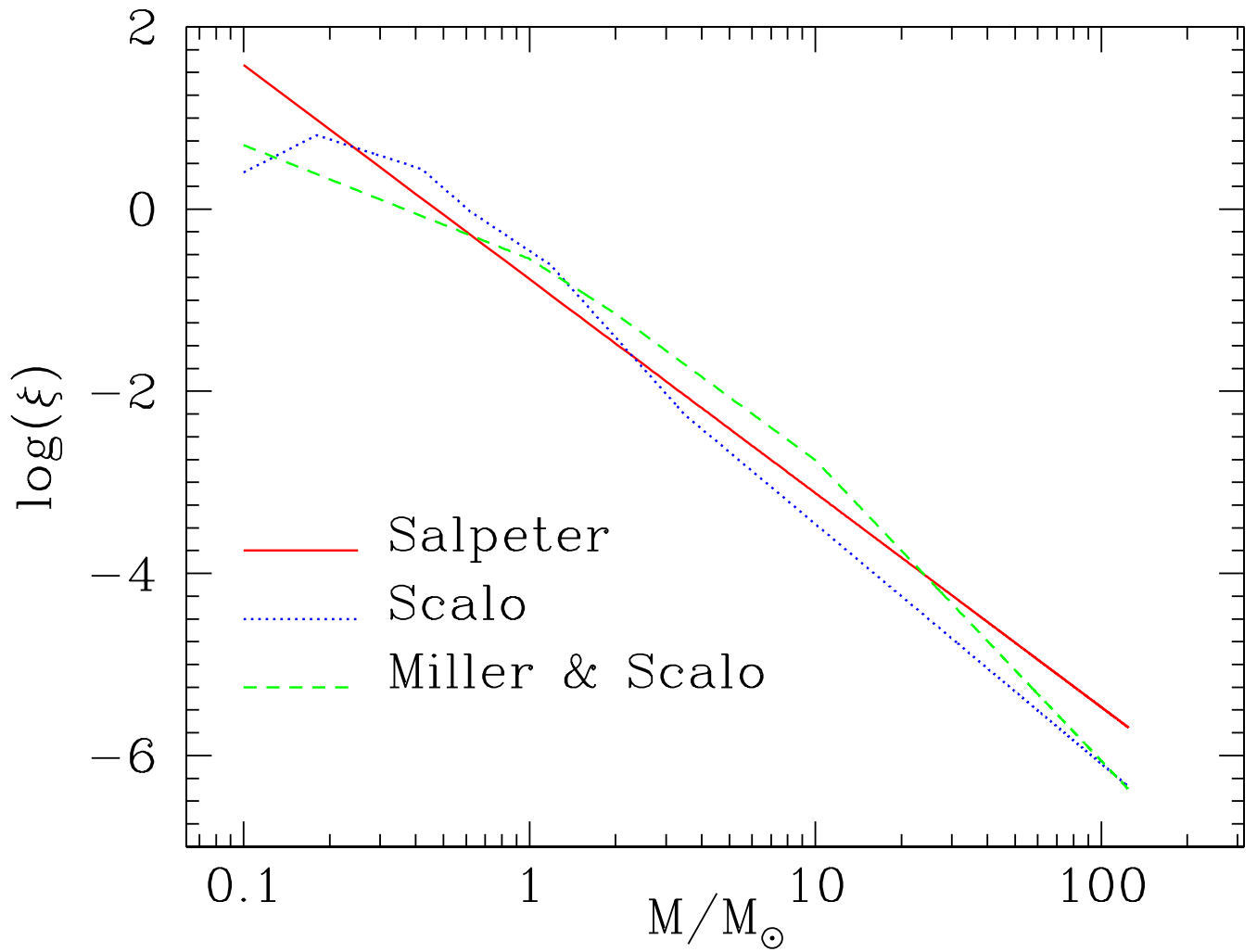


Figure 2: The three IMFs used in the spectral evolutionary models of Bruzual & Charlot (1993).

IMF	M_1	M_2	x
Salpeter	0.10	125.	1.35
Scalo	0.10	0.18	-2.60
	0.18	0.42	0.01
	0.42	0.62	1.75
	0.62	1.18	1.08
	1.18	3.50	2.50
	3.50	125.	1.63
Miller & Scalo	0.10	1.00	0.25
	1.00	2.00	1.00
	2.00	10.0	1.30
	10.0	125.	2.30

Table 1: Parameters of Salpeter (1955), Scalo (1986) and Miller & Scalo (1979) laws for the IMF: M_1 and M_2 are the lower and higher mass cutoffs, and x is the parameter of the power law.

2.2.2 Star Formation Rate

To build a Composite Stellar Population (CSP) we need the birthrate of stars. The Star Formation Rate depends on the amount of gas converted in stars in the galaxy: $\psi(t) = -\frac{df_{\text{gas}}}{dt}$. The Schmidt's (1959) law assumes that the rate of star formation varies with a power n of the density of interstellar gas, $\psi(t) = \psi_0 f_{\text{gas}}^n [M_{\odot}/\text{yr}]$, with $1 \leq n \leq 2$ (see also Tinsley 1980). Assuming $n = 1$ and a closed-box model (constant total mass) with instantaneous recycling of the gas ejected by the stellar remnants, the Schmidt's law leads to the analytic approximation $\psi(t) \propto \exp(-t/\tau)$, also called μ -model, being $\tau = 1/\psi_0$ the timescale. The integrated spectrum of a stellar population with an arbitrary star formation rate $\psi(t)$ can be obtained from the spectrum of a SSP by means of the convolution integral:

$$f_{\text{CSP}}(t) = \int_0^t \psi(t - \tau) f_{\text{SSP}}(\tau) d\tau$$

assuming that the IMF does not change with time. To reproduce the colours of galaxies of different spectral types, we use the parameters of SFR listed in Table 2: the early galaxies can be matched by a delta burst or by an exponentially decaying SFR with $\tau = 1$ Gyr, S0 and Spiral galaxies are well reproduced by a Schmidt law with timescales ranging from 2 and 30 Gyr, and the Irregulars can be represented by a constant SFR.

In Figure 3 we show the evolution of the SEDs for 6 of the considered spectral types. The CSP are built with the GISSSEL98 library, with Miller & Scalo IMF, solar metallicity and different SFRs, as in Table 2. The represented ages range from 10^6 yr to 2×10^{10} yr: we can remark that at the younger ages all the SEDs resemble each other, whereas they start to differentiate at ages $\gtrsim 10^7$ yr, when the 4000 Å break

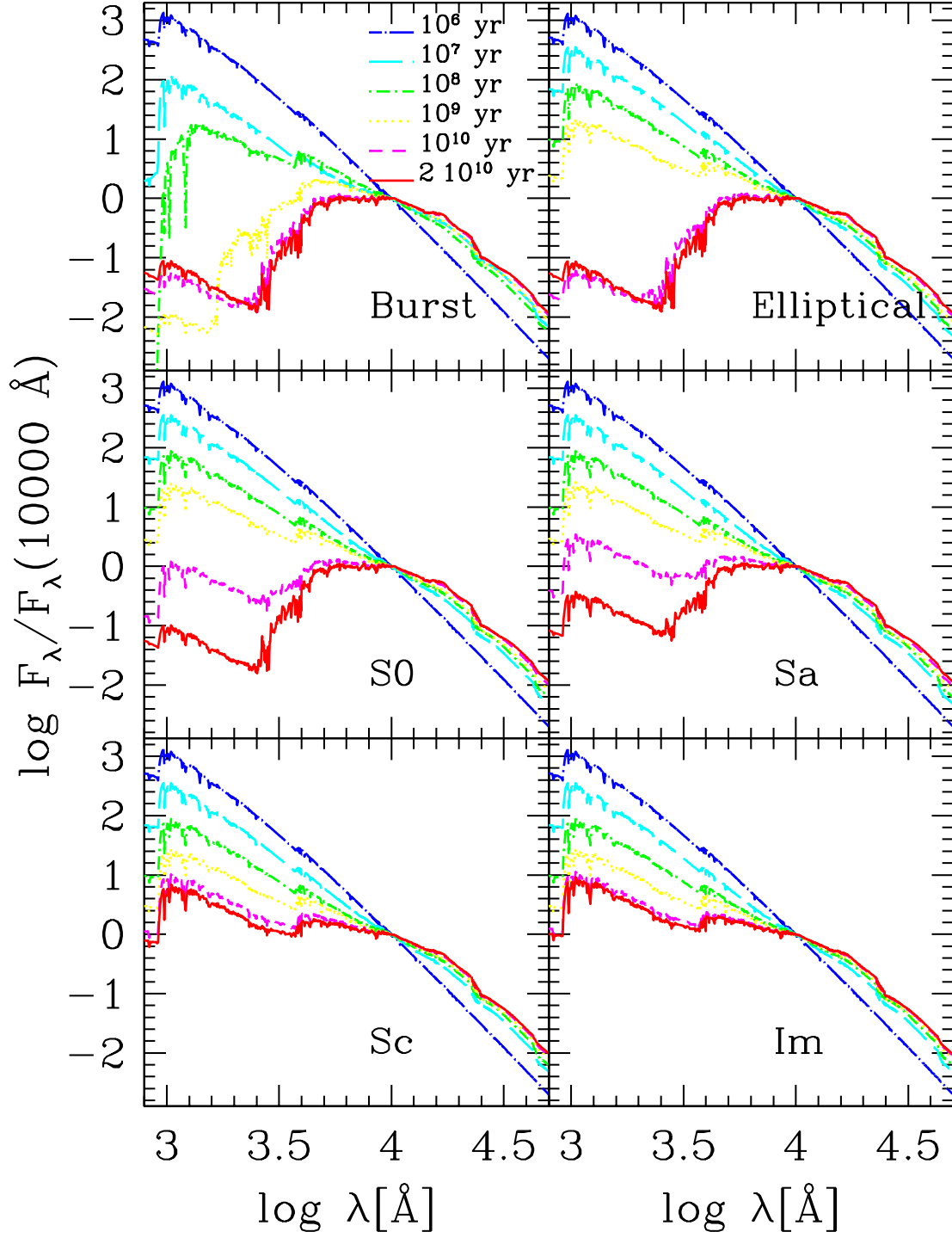


Figure 3: Evolution of the SEDs of different spectral types computed using the spectral evolutionary models of Bruzual & Charlot (1993), with Miller & Scalo IMF, solar metallicity and characteristics of the SFR as shown in Table 1.

file	SpT	SFR	Timescale
./ZPHOT/templates/Burst.ised	Burst	Single Burst	—
./ZPHOT/templates/E.ised	E	Exponential	$\tau = 1$ Gyr
./ZPHOT/templates/S0.ised	S0	Exponential	$\tau = 2$ Gyr
./ZPHOT/templates/Sa.ised	Sa	Exponential	$\tau = 3$ Gyr
./ZPHOT/templates/Sb.ised	Sb	Exponential	$\tau = 5$ Gyr
./ZPHOT/templates/Sc.ised	Sc	Exponential	$\tau = 15$ Gyr
./ZPHOT/templates/Sd.ised	Sd	Exponential	$\tau = 30$ Gyr
./ZPHOT/templates/Im.ised	Im	Constant	—

Table 2: Characteristics of the SFR adopted to match the SEDs of different spectral types of observed galaxies.

becomes detectable. Moreover it is evident that the size of the 4000 Å break is much more conspicuous for earlier types.

2.2.3 Metallicity

The effect of the metallicity parameter is to produce redder colours by increasing the amount of metals contained in the galaxy. Because the same colour effect can be reproduced changing the age or the reddening of the galaxy itself, the metallicity can be regarded as a secondary parameter in the construction of the reference SEDs. Therefore, we decided to use prevalently the synthesis models with a fixed metallicity, set equal to the solar metallicity: $Z = Z_{\odot} \simeq 0.02$, with Z the mass fraction of heavy elements in the interstellar gas.

We explored the effect of considering different extreme metallicities provided by GISSEL98 and template SEDs with metallicity evolution. To this goal we used the approximation of the closed-box model, considering the ejection of heavy elements from each generation of stars, without assuming the instantaneous recycling hypothesis. The tests we carried out (Bolzonella et al. 2000) confirm that the metallicity can be regarded as a secondary parameter. In any case, the files containing SEDs with evolving metallicities can be found in the tar files `zphot_big_endian_evol_MiSc.tar.gz` and `zphot_little_endian_evol_MiSc.tar.gz`. Notice that there will be no SED with metallicity evolution corresponding to the Burst.ised one, because of the nature of the star formation history (an initial single burst followed by a passive evolution).

2.3 Reddening

Recent studies on high redshift galaxies and star formation obscured by dust have shown the importance of the reddening in the high- z universe. Therefore, another

effect that must be taken into account is dust extinction, produced inside the galaxies themselves.

The five reddening laws presently implemented in **hyperz** are:

1. Allen (1976) for the Milky Way (MW);
2. Seaton (1979) fit by Fitzpatrick (1986) for the MW;
3. Fitzpatrick (1986) for the Large Magellanic Cloud (LMC);
4. Prévot et al. (1984) and Bouchet et al. (1985) for the Small Magellanic Cloud (SMC);
5. Calzetti et al. (2000) for starburst galaxies.

The different laws normalized to $k(B) - k(V) = 1$, are presented in Figure 4. The input value is A_V , corresponding to a dust-screen model, with

$$f_{\text{obs}}(\lambda) = f_{\text{int}}(\lambda)10^{-0.4A_\lambda} ,$$

where f_{obs} and f_{int} are the observed and the intrinsic fluxes, respectively. The extinction at a wavelength λ is related to the colour excess $E(B - V)$ and to the reddening curve $k(\lambda)$ by

$$A_\lambda = k(\lambda)E(B - V) = \frac{k(\lambda)A_V}{R_V} ,$$

with $R_V = 3.1$ except for the Small Magellanic Cloud ($R_V = 2.72 \pm 0.21$) and Calzetti's law ($R_V = 4.05 \pm 0.80$).

In detail, Allen's law for the MW is computed from the values of $k(\lambda)/R_V$ tabulated in Table 3. At shorter and longer wavelengths we extrapolate the slope from the last available points. For Seaton's law, we adopt the fit presented by Fitzpatrick (1986), that follows the same relation found by the same author for the LMC:

$$\begin{aligned} \frac{E(\lambda - V)}{E(B - V)} &= C_1 + C_2\lambda^{-1} + \frac{C_3}{\left[\lambda^{-1} - \frac{(\lambda_0^{-1})^2}{\lambda^{-1}}\right] + \gamma^2} \\ &+ C_4 \left[0.539(\lambda^{-1} - 5.9)^2 + 0.0564(\lambda^{-1} - 5.9)^3\right] \end{aligned}$$

with λ in μm . The two laws, for the MW and the LMC, are different in the coefficient values:

	$\lambda_0^{-1}[\mu m^{-1}]$	$\gamma[\mu m^{-1}]$	C_1	$C_2[\mu m]$	$C_3[\mu m^{-2}]$	$C_4[\mu m^{-1}]$
MW	4.595	1.051	-0.38	0.74	3.96	0.26
LMC	4.608	0.994	-0.69	0.89	2.55	0.50

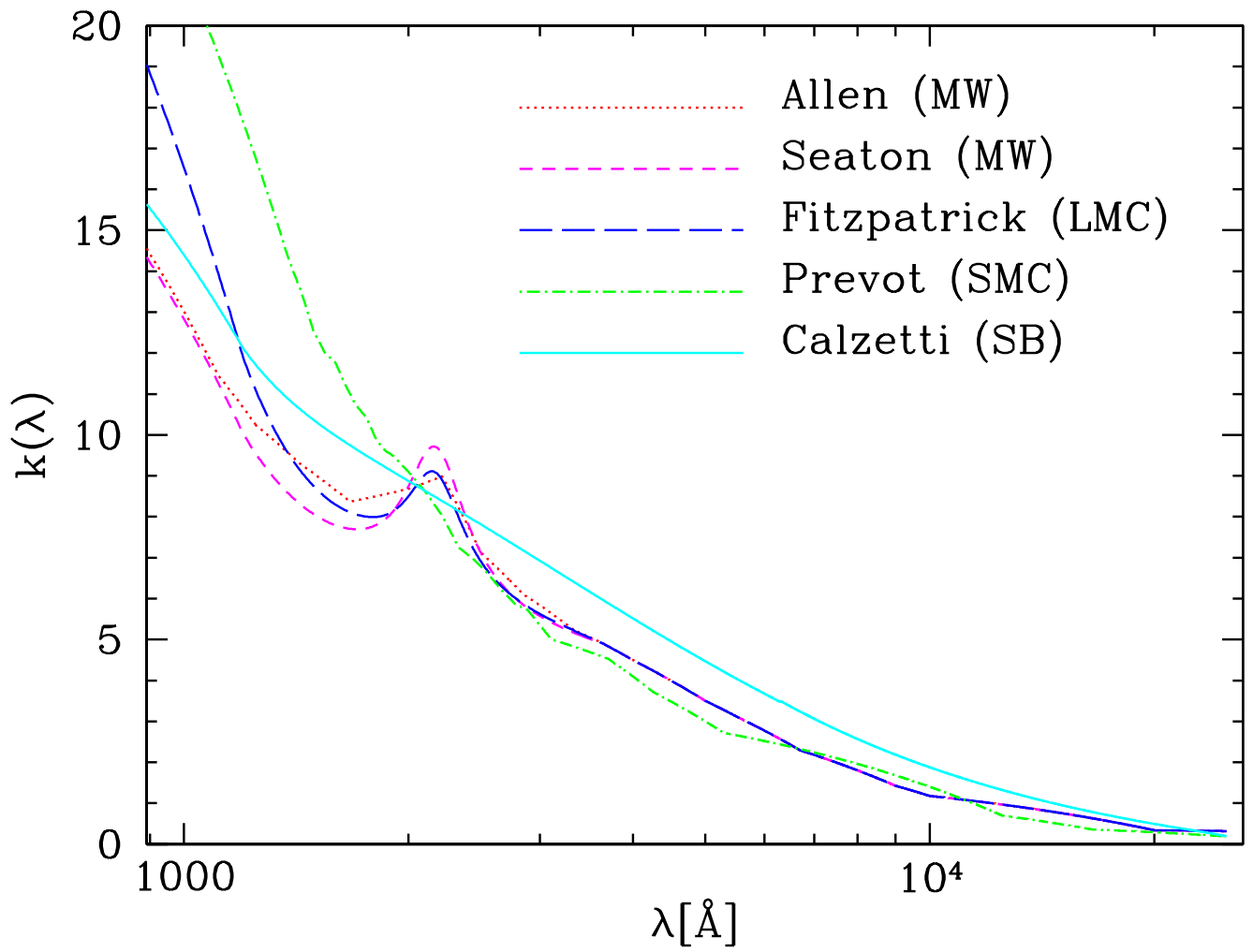


Figure 4: Extinction curves $k(\lambda)$ for the different reddening laws implemented in **hyperz**.

$\lambda[\text{\AA}]$	$k(\lambda)/R_V$	$\lambda[\text{\AA}]$	$k(\lambda)/R_V$	$\lambda[\text{\AA}]$	$\frac{E(\lambda-V)}{E(B-V)}$	$\lambda[\text{\AA}]$	$\frac{E(\lambda-V)}{E(B-V)}$	$\lambda[\text{\AA}]$	$\frac{E(\lambda-V)}{E(B-V)}$
1000.	4.20	3650.	1.58	1275.	13.54	1810.	7.17	2778.	3.15
1110.	3.70	4000.	1.45	1330.	12.52	1860.	6.90	2890.	3.00
1250.	3.30	4400.	1.32	1385.	11.51	1910.	6.76	2995.	2.65
1430.	3.00	5000.	1.13	1435.	10.80	2000.	6.38	3105.	2.29
1670.	2.70	5530.	1.00	1490.	9.84	2115.	5.85	3704.	1.81
2000.	2.80	6700.	0.74	1545.	9.28	2220.	5.30	4255.	1.00
2220.	2.90	9000.	0.46	1595.	9.06	2335.	4.53	5291.	0.00
2500.	2.30	10000.	0.38	1647.	8.49	2445.	4.24	12500.	-2.02
2850.	1.97	20000.	0.11	1700.	8.01	2550.	3.91	16500.	-2.36
3330.	1.69	100000.	0.00	1755.	7.71	2665.	3.49	22000.	-2.47

Table 3: *Left:* Values of $k(\lambda)/R_V$ for the MW reddening law from Allen (1976). *Right:* Values of $E(\lambda - V)/E(B - V)$ for the SMC reddening law from Prévot et al. (1984) and Bouchet et al. (1985).

whereas $C_4 = 0$ for $\lambda^{-1} < 5.9 \mu\text{m}^{-1}$ in any case. Because the validity of these laws is limited to $\lambda^{-1} < 8.3 \mu\text{m}^{-1}$, i.e. $\lambda > 1200 \text{\AA}$, we extrapolated the slope at shorter wavelengths from the 1100 – 1200 \AA range. At wavelengths longer than 3650 and 3330 \AA respectively for the two quoted laws, we adopt the points from Allen, to avoid $k(\lambda)$ being too flat in the red and near-IR regions.

The points used to compute the law for the SMC are taken from Prévot et al. (1984) and Bouchet et al. (1985) and are listed in Table 3. The peculiarity of this law is the lack of the graphite 2175 \AA bump. The non detection of this bump is probably related to the large underabundance of carbon in the SMC. As for Allen’s law, we made an extrapolation from the slope computed from the available points.

The most used attenuation curve in high-redshift studies is the law derived by Calzetti et al. (2000). They derived a law as a purely empirical result from a sample of near starburst (SB) galaxies. Again, the most prominent feature of the MW law is absent: this characteristic suggests that starburst galaxies contain SMC-like dust grains, being the 2175 \AA bump an excellent probe of the type of dust in a galaxy. From Calzetti et al. (2000) we have:

$$k(\lambda) = \begin{cases} 2.659 \left(-2.156 + \frac{1.509}{\lambda} - \frac{0.198}{\lambda^2} + \frac{0.011}{\lambda^3} \right) + R_V & 0.12 \mu\text{m} \leq \lambda \leq 0.63 \mu\text{m} \\ 2.659 \left(-1.857 + \frac{1.040}{\lambda} \right) + R_V & 0.63 \mu\text{m} \leq \lambda \leq 2.20 \mu\text{m} \end{cases}$$

with $R_V = 4.05$. Below the validity wavelength range, we obtain the slope of the reddening law by interpolating $k(\lambda)$ at 1100 and 1200 \AA . In a similar way, we compute the slope at $\lambda > 22000 \text{\AA}$ from the values at 21900 and 22000 \AA .

In particular, the application of this law is suggested for the central star-forming regions of galaxies, and then for high- z galaxies. For this reason, Calzetti’s law is used to correct the value of the SFR at high-redshift, as seen in the previous chapter. It

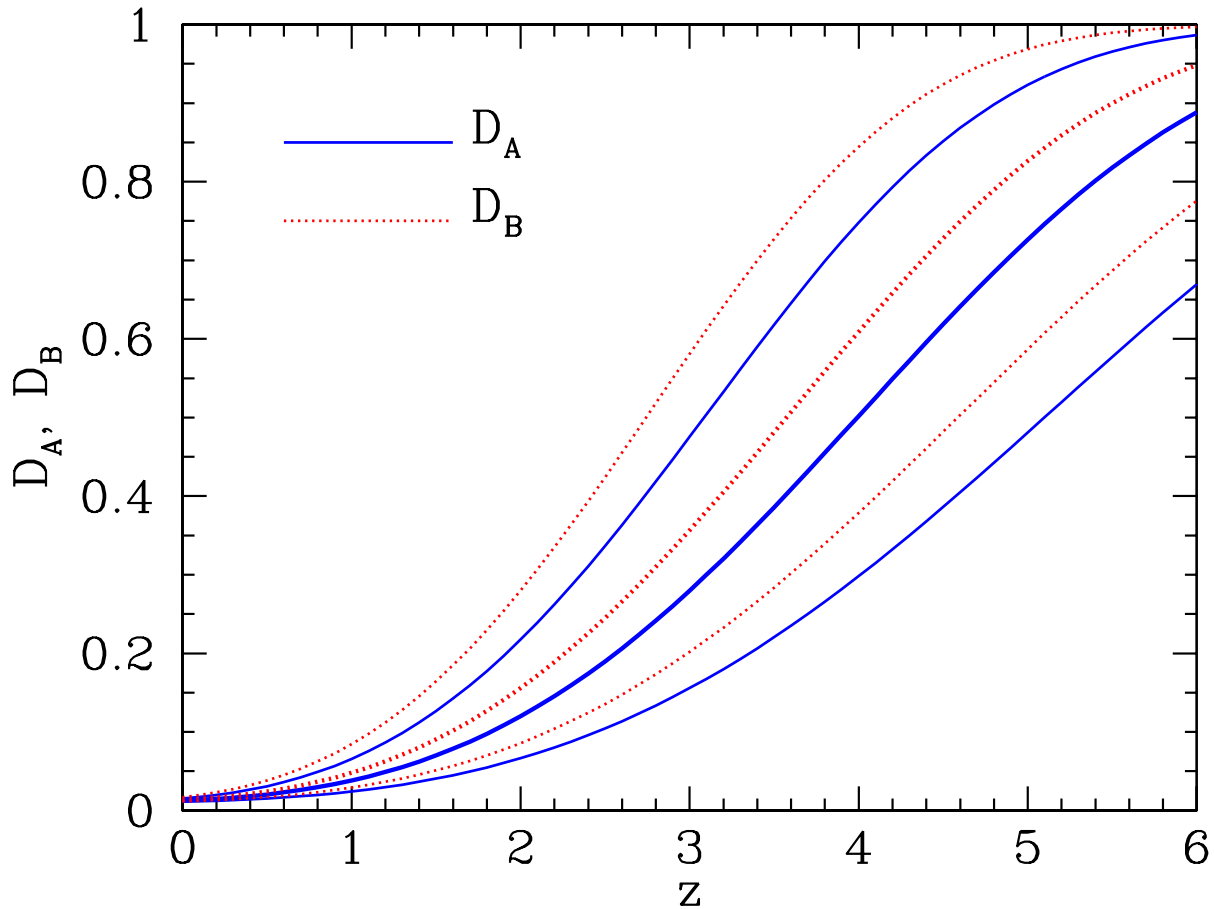


Figure 5: The depression factors D_A and D_B as function of redshift, computed by means of equations 2 and 3 prescribed by Madau (1995), for 3 different values of the optical depth: $0.5\tau_{\text{eff}}^{\alpha,\beta}$ (bottom), $\tau_{\text{eff}}^{\alpha,\beta}$ as defined in Equation 4 (middle), $2\tau_{\text{eff}}^{\alpha,\beta}$ (top).

is evident from Figure 4 that the UV region of the spectrum will be more affected by dust. As a consequence, taking extinction into account is of paramount importance for galaxies at $z \gtrsim 3$, when the rest frame UV emission is shifted to optical wavelengths.

Similarly, but in the opposite way, an extinction curve and a value of the colour excess can be used to deredden the magnitudes of objects seen through the dust of the Milky Way. see next section with parameters description

2.4 Lyman forest

The spectra of high redshift galaxies suffer of a drop in flux below $\text{Ly}\alpha$ at $\lambda = 1216 \text{ \AA}$ and a further decline below $\text{Ly}\beta$, at $\lambda = 1026 \text{ \AA}$. These drops are attributed to absorbing neutral hydrogen clouds at different redshifts between the source and the observer, forming the so-called Lyman forest in the spectra of high redshift objects.

Oke & Korycansky (1982), studying a sample of high redshift QSOs, defined two

depression factors, D_A and D_B , characterizing the amount of absorption between Ly α and Ly β and between Ly β and the Lyman limit respectively: $D_A = 1 - f_{\text{obs}}(\lambda)/f_{\text{int}}(\lambda)$, where $f_{\text{obs}}(\lambda)$ and $f_{\text{int}}(\lambda)$ are the observed and intrinsic fluxes per unit wavelength in the QSO restframe. D_B is defined in the same way as D_A . We adopted the estimates given by Madau (1995) for the attenuation of the continuum due to line blanketing as a function of redshift. He found the flux decrements averaged over all the lines of sight to be

$$\langle D_A \rangle = 1 - \frac{1}{\Delta\lambda_A} \int_{1050(1+z_{\text{em}})}^{1170(1+z_{\text{em}})} \exp(-\tau_{\text{eff}}^\alpha) d\lambda_{\text{obs}} \quad (2)$$

$$\langle D_B \rangle = 1 - \frac{1}{\Delta\lambda_B} \int_{920(1+z_{\text{em}})}^{1015(1+z_{\text{em}})} \exp(-\tau_{\text{eff}}^\beta) d\lambda_{\text{obs}} , \quad (3)$$

$$\tau_{\text{eff}}^\alpha = A_2 \left(\frac{\lambda_{\text{obs}}}{\lambda_\alpha} \right)^{3.46} ; \quad \tau_{\text{eff}}^\beta = \sum_{j=3,11} A_j \left(\frac{\lambda_{\text{obs}}}{\lambda_j} \right)^{3.46} \quad (4)$$

where $\Delta\lambda_A = 120(1 + z_{\text{em}}) \text{ \AA}$ and $\Delta\lambda_B = 95(1 + z_{\text{em}}) \text{ \AA}$. The coefficient A_2 relative to the Ly α forest contribution is equal to 3.6×10^{-3} . The main contribution to $\langle D_B \rangle$, representing the flux decrement caused by all Lyman series lines, belongs to Ly β , Ly γ ($\lambda = 973 \text{ \AA}$) and Ly δ ($\lambda = 950 \text{ \AA}$), whose coefficients are $A_3 = 1.7 \times 10^{-3}$, $A_4 = 1.2 \times 10^{-3}$ and $A_5 = 9.3 \times 10^{-4}$.

Hyperz allow to take into account possible deviation from the average Lyman forest estimated by Madau: in particular it is possible to consider 3 different values of the optical depth $\tau_{\text{eff}}^{\alpha,\beta}$. Figure 5 shows the depression factors D_A and D_B as computed from equations 2 and 3 as well as the flux decrement when the optical depth is multiplied by a factor 0.5 or 2. The fact that $D_B > D_A$ implies that Ly β and higher order lines contribute significantly to line blanketing. We have applied Madau's prescriptions to compute the opacity of IGM through the mean factors $\langle D_A \rangle$ and $\langle D_B \rangle$, whereas we approximated the Lyman continuum absorption setting $f_{\text{obs}}(\lambda) = 0$ for both observed and synthetic SEDs below λ_L , where $\lambda_L = 912 \text{ \AA}$ is the Lyman limit.

3 Hyperz: Getting started

This code was originally developed by Pelló et al. (1996) and Miralles (1998) . Then, it has been improved, generalized, modified to allow a friendly I/O of data and exhaustively tested (Bolzonella et al. 2000) to reach the present public version.

In the following of this section we will describe the procedure followed by **hyperz** and the meaning of all the parameters involved in the computation.

To start, you simply have to type

```
> hyperz
```

and the program will ask you the name of the main parameter file, which default is `zphot.param`:

```
hyperz photometric redshift code - Version 1.2 (October 31, 2000)
by Micol Bolzonella, Roser Pello', Joan-Marc Miralles
More information at http://webast.ast.obs-mip.fr/hyperz/
```

```
Name of parameter file
[default = hyperz.param]
```

After entering the name of your parameter file, or pushing “return” if the name corresponds to the default, the program will notify you the status of input files, i.e. the number of SEDs you required, the number of filters and of objects read from the catalogue and eventually it will report error messages in case of problems reading some input file. For instance:

```
Reading parameter file :
There are 5 synthetic spectra
There are 5 filters
There are 1000 objects in the catalogue
Reading reference sed:
ID: Kurucz's model for Alpha Lyrae. 9400K BB interpolation 1.8-200 microns

There are 3303 points in Vega
Reading synthetic spectra :
Type 1 : /home/mbolzone/ZPHOT/templates/Burst.ised
Type 2 : /home/mbolzone/ZPHOT/templates/E.ised
Type 3 : /home/mbolzone/ZPHOT/templates/Sa.ised
Type 4 : /home/mbolzone/ZPHOT/templates/Sc.ised
Type 5 : /home/mbolzone/ZPHOT/templates/Im.ised
Building hypercube ...
... done
CPU time involved : 170.085 seconds
I'm working ...
Done !!!
Total CPU time involved : 516.522 seconds
```

The hypercube computation (see the next section) will take from some seconds to some minutes, the CPU time depending on your template choice, on the number of redshift and reddening steps, in addition to the clock of your machine.

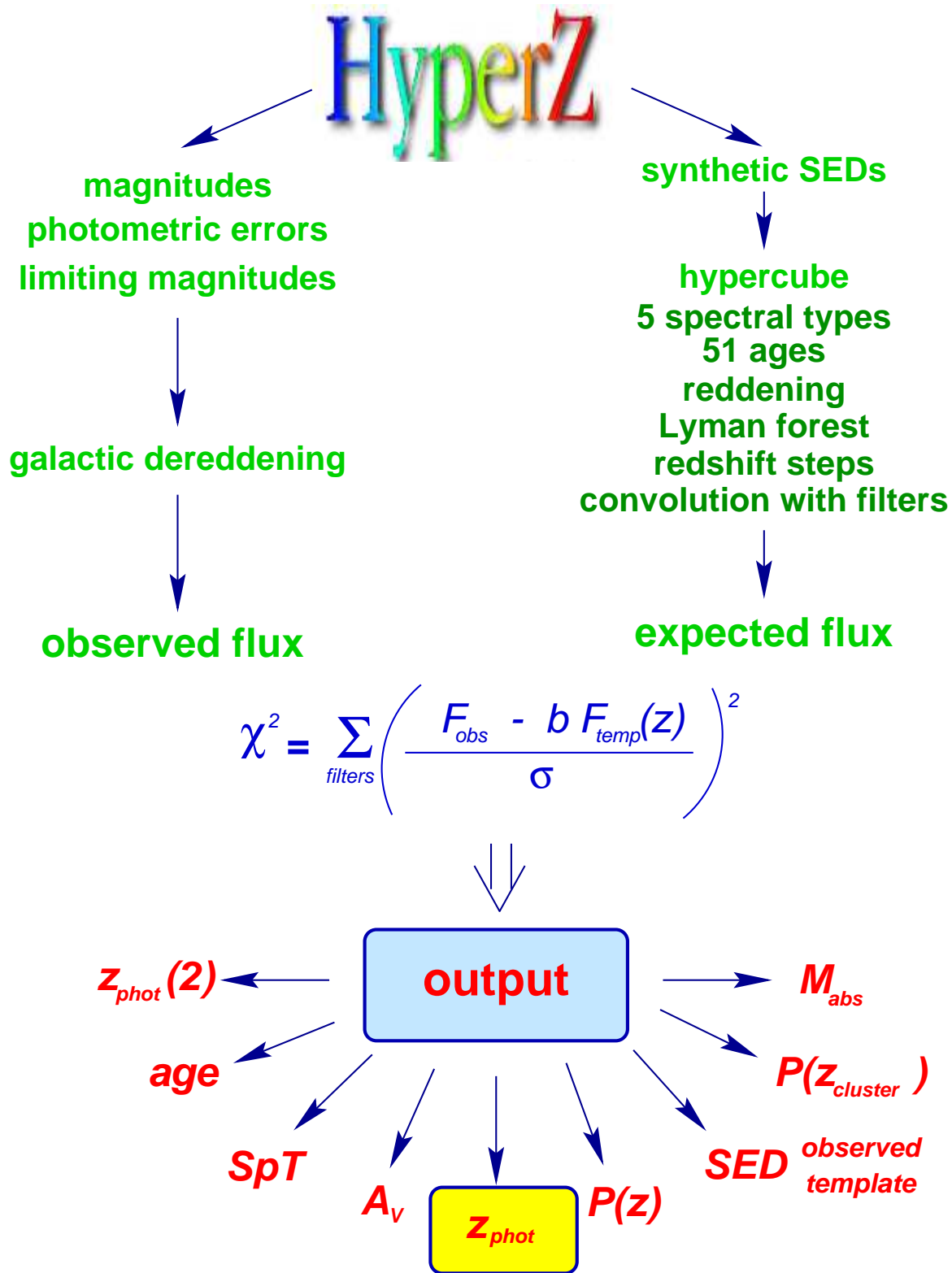


Figure 6: Flow-chart representing how **hyperz** works in its standard configuration.

n	age [Gyr]						
1	0.00032	14	0.02630	27	0.50880	40	8.50000
2	0.00100	15	0.03000	28	0.71870	41	9.50000
3	0.00158	16	0.03300	29	1.01519	42	10.5000
4	0.00251	17	0.03600	30	1.43400	43	11.5000
5	0.00398	18	0.03900	31	1.70000	44	12.5000
6	0.00631	19	0.04500	32	2.00000	45	13.5000
7	0.01000	20	0.05250	33	2.30000	46	14.5000
8	0.01148	21	0.06405	34	2.60000	47	15.5000
9	0.01318	22	0.09048	35	3.50000	48	16.5000
10	0.01514	23	0.12780	36	4.50000	49	17.5000
11	0.01738	24	0.18053	37	5.50000	50	18.5000
12	0.01995	25	0.25500	38	6.50000	51	19.5000
13	0.02291	26	0.36020	39	7.50000		

Table 4: Ages corresponding to the 51 records selected from the 221 available in the GISSEL library.

3.1 Procedure

The procedure followed in the code **hyperz** is illustrated in Figure 6. The first step consists in reading the observed magnitudes, with the corresponding errors and the limiting magnitudes for non detected objects. Take care that to obtain reliable results, the photometry must be carried out in all filters within the same aperture, i.e. the flux must belong to the same physical region. If requested, a dereddening for the Galactic extinction is applied to the photometric catalogue. Hence the magnitudes and the errors are transformed in fluxes. On the other side, there is the handling of the template SEDs. The program builds an *hypercube*, consisting of the fluxes derived from the reference spectra in the following way. If the spectra are taken from the GISSEL library they consist of 221 age records. To save CPU time and memory, **hyperz** provides a rebinning, to reduce the number of considered ages to 51, with the values showed in Table 4. In the “standard” configuration 5 spectral types are considered, corresponding to the Burst, E, Sa, Sc and Im illustrated in the previous section. More SEDs can be redundant. The spectra are reddened following an extinction law chosen from those listed in Section 2.3, and then depressed with the Lyman forest, according to the considered redshift step and to the 3 possible values of the optical depth. At this point, the spectra are convolved with the filter response functions (plus detector if needed, see Section A), to obtain the expected fluxes.

After the *hypercube* construction, the program proceeds with the χ^2 calculation, considering all redshifts, spectral types, ages and absorption values. Minimizing the reduced χ^2 the program finds the better photometric redshift solution and the corre-

sponding SED. Different output files can be chosen by the user, containing different informations, as the best z_{phot} , the observed SEDs (mean fluxes and errors), the best-fit integrated SEDs and spectra, the minimum χ^2 as a function of redshift and the secondary solutions.

3.2 Parameters

In this section we will describe in detail the input and output files involved in the procedure of **hyperz**, with an exhaustive description of all parameters contained in `hyperz.param` and an example of these files.

3.2.1 Inputs

The file `hyperz.param` contains the following input parameters common in **hyperz** and **make_catalog** and those used only in **hyperz**; the parameters used only in **make_catalog** will be described in Section 4.

Common parameters:

- **AOVSED**: the file-path containing the spectrum of Vega;
- **FILTERS_RES**: the file-path containing the filter transmission functions;
- **FILTERS_FILE**: the file containing information about filters. The first column is the identification number of each filter in the file `FILTER.RES`. The user can check it in the file `filters.log` (see Section A). If the user wants a combination of several filters, e.g. n_1 (filter) and n_2 (detector), write $n_1\&n_2$ in the first column. When the magnitude system is different from the standard Vega or AB, the second column contains the correction (in magnitudes): $m_{\text{Vega}} = m_{\text{cat}} + m_{\text{corr}}$. When the magnitude system is the standard Vega or AB, $m_{\text{corr}} = 0$. The user can specify the magnitude system AB using the **MAG_TYPE** parameter. See Fukugita et al. (1995) for typical correction values. Also, when using the Thuan-Gunn system (based on the standard BD+17 4708):

$$\begin{aligned}
 g(\text{Vega}) &= g(\text{TG}) + 0.201 \\
 r(\text{Vega}) &= r(\text{TG}) - 0.401 \\
 i(\text{Vega}) &= i(\text{TG}) - 0.672 \\
 z(\text{Vega}) &= z(\text{TG}) - 0.762
 \end{aligned}$$

The third column is the rule applied in the case of undetected objects:

- **0**. This filter will not be taken into account in the computation.

1. The flux in this filter is set to $F_{\text{obs}} = 0$ with an error corresponding to the flux deduced from the limiting magnitude in the fourth column, i.e. $\Delta F_{\text{obs}} = F_{\text{lim}}$.
2. The flux in this filter and the associated 1σ error are set equal to $F_{\text{lim}}/2$.
3. The flux in this filter and the associated error are computed from the limiting magnitude m_{lim} and from the error Δm_{lim} given in columns four and five, respectively.

Undetected objects in a filter i are characterized by a magnitude $m(i) > 90$ [in general $m(i) = 99$, following the convention of the photometric software **SExtractor** (Bertin & Arnouts 1996)]. “Out of field” objects, for which the photometry is not available, must be characterized by a magnitude $m(i) < 1$ (in general $m(i) = 0$); in this way the filter “out of field” is not taken into account in the χ^2 minimization procedure.

The fourth column gives the limiting magnitude $m_{\text{lim}}(i)$ in each filter i . The fifth column is the error value in magnitudes, $\Delta m_{\text{lim}}(i)$, that will be attributed to undetected objects when option 3 is selected in column three. Lines beginning with a $\#$ or blank lines are not considered.

- **TEMPLATES_FILE**: the name of the file containing the path of templates that the user wants to use and their type (**BC** = Bruzual & Charlot, binary, **AS** = ASCII); the user can select or unselect a template by placing or removing a $\#$ as the first character in the `spectra.param` file. The correct path of templates must be checked by the user.

The present library consists of 8 synthesis template SEDs with solar metallicity and Miller & Scalo IMF presented in Section 2.2.1, and 4 spectra from CWW and extended in UV and near-IR with the GISSEL98 library. This set of templates can be changed by the user.

- **MAG_TYPE**: the type of magnitude used in the catalogue: 0 for standard magnitudes (Vega system or others, see **FILTERS_FILE**), 1 for AB magnitudes. Output absolute magnitudes will be of the same type.
- **ERR_MAG_MIN**: in **hyperz** this is the value of the photometric error which is set if the input error from the catalogue is $< \text{ERR_MAG_MIN}$, to avoid too small and non-realistic photometric errors. It is worth to note that SEDs computed from a catalogue are “absolute”, in the sense that errors should include ALL the possible sources (air-mass, photometric zero-points, background noise, etc.). In **make_catalog** this error is a kind of zeropoint error, added quadratically to the error estimate. See the description of the parameter **NOISE_TYPE** in Section 4.

- **Z_MIN** and **Z_MAX**: the limits of the redshift range the user wants to investigate. In **hyperz** These parameters are connected to **CATALOG_TYPE**: if **CATALOG_TYPE** = 0, these limits are set for all the objects in the catalogue; if **CATALOG_TYPE** = 1, the limits are set individually for each object. In **make_catalog** they identify the range where the redshift of the simulated galaxies z have to be selected.
- **REDDENING_LAW**: the law for internal reddening (see Section 2.3):
 0. No reddening
 1. MW from Allen (1976);
 2. MW from Seaton (1979);
 3. LMC from Fitzpatrick (1986);
 4. SMC from Prévot et al. (1984) and Bouchet et al. (1985);
 5. Starburst galaxies from Calzetti et al. (2000).
- **AV_MIN**, **AV_MAX**: the values of the maximum and minimum absorption in the V band (in magnitudes). If **REDDENING_LAW** = 0, these values are not taken in account.
- **LY_FOREST**: option for the Lyman forest flux decrement: if **LY_FOREST** = 1. the optical depth of the neutral hydrogen is set equal to the average value given by Madau (1995); if **LY_FOREST** \neq 1. other two values of τ_{eff} will be considered $\tau_{\text{eff}}/\text{LY_FOREST}$ and $\tau_{\text{eff}}*\text{LY_FOREST}$
- **OUTPUT_FILE**: the name of output files (without extension). In **hyperz** the output files will have the extensions **.out_phot**, **.z_phot**, **.cat_phot**, **.log_phot**, **.obs_sed** and **.temp_sed**; in **make_catalog** **.model** and **.cat** (see Section 4).
- **H0**: the Hubble constant; used in **hyperz** if the age check is switched on and for absolute magnitude computation.
- **OMEGA_M**: the matter density parameter; used in **hyperz** if the age check is switched on and for absolute magnitude computation.
- **OMEGA_V**: the cosmological constant density parameter; used in **hyperz** if the age check is switched on and for absolute magnitude computation.

Hyperz only parameters:

- **FILT_M_ABS**: the filter number (to be checked in the file **filters.log**, as before) for the absolute magnitude estimate, taking into account the k -correction computed using the best fit SED. The absolute magnitude will be of the same type of input magnitudes, following the parameter **MAG_TYPE**.

- **CATALOG_FILE**: the name of the input photometric catalogue.
- **CATALOG_TYPE**: must be set to 0 if the input catalogue has the format:

$$\text{id}, [m(i), i = 1, n_{\text{filt}}], [\Delta m(i), i = 1, n_{\text{filt}}]$$
 where **id** is the identification number, $m(i)$ are the observed magnitudes, $\Delta m(i)$ are the corresponding photometric errors and n_{filt} the number of filters. **CATALOG_TYPE** must be set to 1 if the format is

$$\text{id}, z_{\text{min}}, z_{\text{max}}, [m(i), i = 1, n_{\text{filt}}], [\Delta m(i), i = 1, n_{\text{filt}}]$$
 with a redshift range ($z_{\text{min}}, z_{\text{max}}$) that can be different for each object. In the latter case the values of **Z_MIN** and **Z_MAX** are not taken in account.
- **Z_STEP**: the step in redshift used in the first estimate of best fit. After the first minimization, the candidate solutions are refined with a step $\text{Z_STEP}/10$ to search for smaller χ^2 .
- **ZSTEP_TYPE**: the option for the type of step in redshift: if **ZSTEP_TYPE** = 0 the step is constant and equal to **Z_STEP**, if **ZSTEP_TYPE** = 1 the step is evolving as $\text{Z_STEP} \times (1 + z)$. The latter is preferable if the user wants to better investigate the low redshifts region without increasing the total number of steps and consequently the CPU time.
- **AV_STEP** the value of the computation step to cover the range defined by **AV_MIN** and **AV_MAX**.
- **AGE_CHECK**: the option for the control of age as a function of redshift: if this parameter is set equal to **y** or **Y** the program checks that the age of the template is less than the age of the universe (for a cosmological model assigned with **H0**, **OMEGA_M** and **OMEGA_V**) at the redshift under consideration.
- **PROB_THRESH**: the minimum value of the probability (inferred from the reduced χ^2 analysis) for the study of secondary maxima. The range of permitted values is 0 – 100.
- **OUTPUT_TYPE** : selects the flux units for the output SEDs in files with extension **.spe**, **.temp_sed** and **.obs_sed**:
 0. $2 \times 10^{-17} \text{erg/cm}^2/\text{s}/\text{\AA}$;
 1. μJy ;
 2. AB magnitudes.
- **SED_OBS_FILE**, **SED_TEMP_FILE**, **LOGPHOT_FILE**, **ZPHOT_FILE** and **CATPHOT_FILE** are the options **y/n** for the output files containing:

ν	$P = 0.99$	0.95	0.90	0.75	0.68	0.50
1	0.00016	0.00393	0.0158	0.1015	0.170	0.455
2	0.0100	0.0515	0.105	0.288	0.386	0.693
3	0.0383	0.117	0.195	0.404	0.503	0.789
4	0.0742	0.178	0.266	0.481	0.576	0.839
5	0.111	0.229	0.322	0.535	0.626	0.870
6	0.145	0.273	0.367	0.576	0.663	0.891
7	0.177	0.310	0.405	0.608	0.691	0.907
8	0.206	0.342	0.436	0.634	0.713	0.918
9	0.232	0.369	0.463	0.655	0.732	0.927
10	0.256	0.394	0.487	0.674	0.747	0.934

Table 5: Values of the reduced χ^2 corresponding to the probability $P(\chi^2|\nu)$ of exceeding the value χ^2 by chance, as a function of the number of degrees of freedom ν .

- `OUTPUT_FILE.obs_sed`: the observed SEDs, given as the mean integrated fluxes through the photometric system, and the corresponding errors (units selected by `OUTPUT_TYPE`).

$$\text{id}, [F_{\text{obs}}(i), i = 1, n_{\text{filt}}], [\Delta F_{\text{obs}}(i), i = 1, n_{\text{filt}}]$$

- `OUTPUT_FILE.temp_sed`: the best fit integrated SEDs (same units).

$$\text{id}, [F_{\text{temp}}(i), i = 1, n_{\text{filt}}]$$

- `OUTPUT_FILE.log_phot`: the best fit parameters as a function of the redshift, with steps defined by `Z_STEP`:

$$\text{id}, z_{\text{step}}, \chi_{\nu}^2(z_{\text{step}}), P(\chi_{\nu}^2), \text{SpT}, \text{age [Gyr]}, A_V, \text{Ly forest}$$

where z_{step} is the redshift step, $\chi_{\nu}^2(z_{\text{step}})$ is the minimum reduced χ^2 corresponding to the considered redshift, $P(\chi_{\nu}^2)$ is the probability associated to the value of χ_{ν}^2 and the degrees of freedom involved (see Table 5), `SpT`, `age [Gyr]` and A_V are the spectral type, the age and the reddening of the SED corresponding to the minimum χ^2 . `Ly forest` is the factor multiplying the optical depth of the neutral hydrogen defined in Equation 4 and producing the minimum χ^2 . The χ_{ν}^2 is defined by χ^2/ν , where ν is the number of degrees of freedom. Because we are interested in only one parameter (the photometric redshift), the degrees of freedom are $n_{\text{filt}} - 1$, subtracting the degree of freedom lost with the normalization b in equation 1.

- `OUTPUT_FILE.z_phot`: the best fit redshift and corresponding parameters for each object:

$$\text{id}, z_{\text{phot}}, \chi_{\nu}^2, P(\chi^2), \text{SpT}, N_{\text{age}}, \text{age [Gyr]}, A_V, b, z_{\text{inf}}(99\%), z_{\text{sup}}(99\%), z_{\text{inf}}(90\%), z_{\text{sup}}(90\%), z_{\text{inf}}(68\%), z_{\text{sup}}(68\%), z_{\text{wm}}, P(\chi_{\text{wm}}^2), M_{\text{abs}}, \text{Ly forest}, z_{\text{phot}}(2), P[\chi^2(2)]$$

where z_{phot} is the redshift corresponding to the minimum χ^2 , N_{age} is the age record number, as listed in Table 4, followed by the other SED characteristics corresponding to the best fit spectrum. z_{inf} and z_{sup} are the extrema of confidence intervals defined by the $\Delta\chi^2$ method, being the number of “interesting parameters” equal to 1, i.e. the photometric redshift. In this case the values of $\Delta\chi^2$ defining the confidence intervals at 99%, 90% and 68% are 1.00, 2.71 and 6.63 respectively (Avni 1976). The other quantities are the weighted mean z_{wm} , computed in the confidence interval at 99% around the main solution, the associated probability, the absolute magnitude M_{abs} in the `FILT_M_ABS` filter. `Ly forest` is the factor multiplying the neutral hydrogen optical depth. $z_{\text{phot}}(2)$ and $P[\chi^2(2)]$ are the secondary solution and its χ^2 probability.

If the user switches on the `Z_CLUSTER` option three columns are added: the absolute magnitude in the `FILT_M_ABS` filter if the object is at `Z_CLUSTER`, the probability at `Z_CLUSTER` and the apparent magnitude in the redshifted filter closest to `FILT_M_ABS` (used to estimate the absolute magnitude).

- `OUTPUT_FILE.cat_phot`: the best fit and secondary solutions (if any) for each object. `CATPHOT_FILE` contains `ZPHOT_FILE`, and it has the same format, without the columns regarding the secondary solution and the cluster option, and with an additional column to display the solution rank.

Note that looking at the `OUTPUT_FILE.log_phot` file the user can find that the secondary maximum has a higher probability than the first one. This is because of the refinement around the χ^2 minima: the main photometric redshift and the secondary solution are written after the refinement, whereas the file `OUTPUT_FILE.log_phot` contains probabilities before the refinement, with the step `Z_STEP`. After refinement, some solutions can change their rank in the solution classification.

- `Z_CLUSTER`: optional parameter; if the user selects this option, the program computes the probability of each object to lie at `Z_CLUSTER` and writes it in the `.z_phot` file.
- `M_ABS_MIN`: optional parameter; the minimum absolute magnitude (bright), it must be of the same type selected in `MAG_TYPE`.
- `M_ABS_MAX`: optional parameter; the maximum absolute magnitude (faint), it must be of the same type selected in `MAG_TYPE`.

- **MATRIX**: optional parameter. The user can choose **y/Y** or **n/N** (default is **n**): if the user selects **y/Y** the program will write for each object a file **#id.m** containing the χ^2 value over the parameter space:

$$\text{id, } z, \text{ SpT, } N_{\text{age}}, \text{ age [Gyr], } A_V, \text{ Ly forest, } \chi^2.$$

If the catalogue contains more than 100 objects the program asks to confirm, because these are large files.

- **SPECTRUM**: optional parameter as **MATRIX**. If the user chooses **y/Y** (default is **n**), files named **#id.spe** containing the spectrum of the best fit model $\lambda, F(\lambda)$ are written for each galaxy.
- **EBV_MW**: optional parameter. The colour excess $E(B - V)$ for the galactic dereddening of data (default is **EBV_MW** = 0). The reddening law used for the dereddening is number 1 (Allen 1976).

The file **OUTPUT_FILE.out_phot** is a fixed output, summarizing the main parameters used running **hyperz**:

- the name of the photometric catalogue file;
- the name and associated number of template files;
- the characteristics of filters:
 - **n** is the number of filter in the file **FILTER.RES**;
 - **wl_eff** is the effective wavelength of the filter, computed as:

$$\lambda_{\text{eff}} = \frac{\int \lambda R(\lambda) d\lambda}{\int R(\lambda) d\lambda},$$

where $R(\lambda)$ is the filter transmission normalized at $R_{\text{max}} = 1$;

- **surface** is the integral of the normalized filter transmission:

$$S = \int R(\lambda) d\lambda;$$

- **bandpass1** is the effective bandpass computed with a Gaussian approximation:

$$\Delta\lambda = 2\sqrt{\frac{\int (\lambda - \lambda_{\text{eff}})^2 R(\lambda) d\lambda}{S}};$$

- **conv_AB** is the conversion between AB and Vega magnitudes (see Section A):

$$m_{\text{Vega}} = m_{\text{AB}} - \text{conv_AB};$$

- mag_lim is the limiting magnitude (selected in FILTERS_FILE);
- nd is the non detection law (selected in FILTERS_FILE);
- the range and step in redshift;
- the range and step in A_V and reddening law;
- the range of absolute magnitudes and the filter used to compute it;
- the cosmological parameters.

The user must check the maximum number of steps in redshift and reddening and the maximum number of templates and filters in the file `~/ZPHOT/src/dimension.dec`. The program will stop if the user requests a number exceeding the maximum. If the user wants to change some dimensions (because of problems of memory in the user's machine if the size of the executable is too large or if the user wants to increase the array dimensions), he/she must edit the file and recompile the program.

Here we report an example of the parameter files `hyperz.param`, `UBVRI.param`, `spectra.param` and of the photometric catalogue `UBVRI.cat`:

```

:~::~:
hyperz.param
:~::~:
#####
##### hyperz & make_catalog parameters #####
##### version 1.2 - October 31, 2001 #####
##### by Bolzonella, Pello' & Miralles #####
#####
#### Reference: Bolzonella, Miralles & Pello', 2000, A&A 363, 476 ####
#### Web:      http://webast.ast.obs-mip.fr/hyperz/      ####
#####

AOVSED      ~/ZPHOT/filters/AOV_KUR_BB.SED # Vega SED
FILTERS_RES ~/ZPHOT/filters/FILTER.RES  # filters' transmission
FILTERS_FILE ~/ZPHOT/filters/UBVRI.param # filters' file
TEMPLATES_FILE spectra.param          # models file
MAG_TYPE    0                          # 0: standard Vega magnitudes
                                           # 1: AB magnitudes (Oke 1974)
ERR_MAG_MIN 0.05                        # minimum photometric error
                                           # (used in make_catalog if NOISE_TYPE=1)
Z_MIN       0.00                        # minimum redshift
Z_MAX       6.00                        # maximum redshift
REDDENING_LAW 5                          # reddening law
                                           # 0 no reddening
                                           # 1 Allen (1976) MW
                                           # 2 Seaton (1979) MW
                                           # 3 Fitzpatrick (1983) LMC
                                           # 4 Prevot (1984) Bouchet (1985) SMC

```

```

# 5 Calzetti (2000)
AV_MIN      0.0      # minimum A_v
AV_MAX      1.2      # maximum A_v
LY_FOREST   1.0      # Lyman Forest
# 1. : fixed Madau value
# other values: 3 optical depths considered
# <tau_eff>/LY_FOREST, <tau_eff> and
# <tau_eff>*LY_FOREST
OUTPUT_FILE  UBVRT   # N.B. no extension !!
# hyperz: root name for output files
# (see other parameters)
# make_catalog: .model random catalogue
# .cat catalogue with noise
HO          50.      # Hubble constant in Km/s/Mpc
OMEGA_M     1.       # density parameter (matter)
OMEGA_V     0.       # density parameter (Lambda)
##### hyperz only #####
FILT_M_ABS  91       # filter for absolute magnitude
CATALOG_FILE ~/ZPHOT/models/UBVRT.cat # catalogue file
CATALOG_TYPE 0       # cat.type
# 0 z/cat
# 1 z/obj
Z_STEP      0.05    # step in redshift
ZSTEP_TYPE  0       # 0 step = Z_STEP
# 1 step = Z_STEP*(1+z)
AV_STEP     0.20    # Av_err
AGE_CHECK   y       # check age gal. < age universe
PROB_THRESH 10.00   # prob. thresh. for second. max. (0,100)
OUTPUT_TYPE 0       # 0 2.E-17 erg/cm^2/s/A, 1 microJy, 2 mag_AB
SED_OBS_FILE n      # file .obs_sed
SED_TEMP_FILE n     # file .temp_sed
LOGPHOT_FILE n     # file .log_phot
CATPHOT_FILE n     # file .cat_phot
ZPHOT_FILE  y      # file .z_phot
# ages if AGE_CHECK = y
##### optional parameters #####
#Z_CLUSTER  1.      # redshift of cluster
#M_ABS_MIN  -28.    # minimum absolute magnitude (bright)
#M_ABS_MAX  -9.     # maximum absolute magnitude (faint)
MATRIX      n      # file .m for each object
SPECTRUM    n      # file .spe for each object
EBV_MW      0.     # E(B-V) for galactic dereddening
##### make_catalog only #####
REF_FILTER  113     # reference filter
MAG_MIN     22.    # minimum apparent magnitude in REF_FILTER
MAG_MAX     25.    # maximum apparent magnitude in REF_FILTER
NOISE_TYPE  1      # 0: random noise with fixed sigma in mag
# 1: noise dm(m)
N_OBJ       1000   # number of objects
Z_FORM      10.    # formation redshift
AGE_RANDOM  0      # 0 age = age of universe - T(z_form)
# 1 age = random in [0,T(z)-T(z_form)]
RAND_SEED   3010   # seed for random generator (max 4 figures)

```

#####

.....

UBVRI.param

.....

12	0.00	1	29.5	0.5
108	0.00	1	30.0	0.5
111	0.00	1	30.0	0.5
112	0.00	1	30.0	0.5
113	0.00	1	30.0	0.5

.....

spectra.param

.....

~/ZPHOT/templates/Burst.ised	BC
~/ZPHOT/templates/E.ised	BC
#~/ZPHOT/templates/S0.ised	BC
~/ZPHOT/templates/Sa.ised	BC
#~/ZPHOT/templates/Sb.ised	BC
~/ZPHOT/templates/Sc.ised	BC
#~/ZPHOT/templates/Sd.ised	BC
~/ZPHOT/templates/Im.ised	BC
#~/ZPHOT/templates/CWW_E.ext.sed	AS
#~/ZPHOT/templates/CWW_Sbc.ext.sed	AS
#~/ZPHOT/templates/CWW_Scd.ext.sed	AS
#~/ZPHOT/templates/CWW_Im.ext.sed	AS

.....

UBVRI.cat

.....

1	24.660	25.239	24.588	23.581	22.745	0.051	0.052	0.051	0.050	0.050
2	99.000	99.000	29.498	25.686	23.100	1.000	1.000	0.336	0.054	0.050
3	28.018	27.582	25.930	25.241	24.309	0.175	0.122	0.056	0.051	0.050
4	28.524	26.291	24.674	24.140	23.493	0.349	0.060	0.051	0.050	0.050
5	99.000	99.000	27.048	25.204	24.048	1.000	1.000	0.087	0.052	0.050

3.2.2 Outputs

The quantities provided as outputs of **hyperz** have been already described in the previous section. Here we report an example of the `.z_phot` file:

.....

UBVRI.z_phot

.....

1	0.54000	0.157	96.00	5	35	3.5000	1.00	0.154E-06	0.450	0.717	...	-18.59	1.000	0.645	93.21
2	5.15000	0.001	100.00	1	18	0.0390	0.00	0.714E+01	4.925	5.478	...	-23.16	1.000	5.300	100.00
3	0.14500	0.563	68.96	1	31	1.7000	1.20	0.211E+03	0.000	0.317	...	-13.23	1.000	1.935	0.02
4	3.19000	0.039	99.72	5	27	0.5088	1.00	0.249E-06	2.947	3.345	...	-22.94	1.000	2.505	73.51
5	4.25000	0.000	100.00	2	28	0.7187	1.20	0.338E+03	3.941	4.740	...	-23.60	1.000	4.500	100.00

As stated above, the format of this file is the following, ordered by columns: (1) the identification number; (2) the photometric redshift primary solution; (3) its χ^2_V and (4) the corresponding probability; (5) the number of the spectral type in the order of the `spectra.param` file; (6) the age record; (7) the age in Gyr; (8) the absorption in the V band to be applied at the best fit SED; (9) the normalization factor b of equation 1 needed to minimize the χ^2 ; (10)-(11), (12)-(13) and (14)-(15) the limits of the confidence intervals at 99%, 90% and 68%; (16) the weighted mean redshift z_{wm} ; (17) the probability associated to z_{wm} (the columns 12 – 17 here are replaced by dots); (18) the absolute magnitude; (19) the factor multiplying the optical depth of the Lyman forest; (20) the secondary peak of the probability function; (21) the probability of the secondary solution.

One of the most considerable features of **hyperz**, is the possibility of knowing the probability function $P(z)$. This characteristic allows us to describe in an accurate way the results of different tests and to explore the relevance of secondary solutions and then the degeneracy in the parameter space. Moreover, the function $P(z)$ can be used to compute some cosmological quantities properly taking into account the characteristics of the photometric redshift technique. Figure 7 shows an example of SED fitting and the corresponding $P(z)$ for three objects.

4 Make_catalog: Getting started

The public version of the package **hyperz** contains also the program **make_catalog**, useful to build simulated catalogues and to study the accuracy of photometric redshifts as a function of different parameters. The plots in the cover of this manual are an example of this kind of application. Basically, **make_catalog** compute magnitudes using the same template SEDs previously described, and then photometric errors are introduced as Gaussian noise. After a successful installation, the program can be called simply typing `make_catalog` and writing the name of the main parameter file, called by default `hyperz.param`. In the new version this parameter file is the same of that used by **hyperz**, because of the large number of common parameters.

4.1 Parameters

The input parameters used by **make_catalog**, contained in `hyperz.param` and different from **hyperz** are:

- **FILTERS_FILE**: the name of the file containing in the first column the identification of filters and in the following columns the information needed to compute photometric errors, according to the error type selected by the parameter **NOISE_TYPE**.

In this file lines beginning with a `#` are not considered.

- **OUTPUT_FILE**: the output files created by **make_catalog** will be named `OUTPUT_FILE.model`, containing random catalogue obtained from the templates, with format


```
id, z, SpT, age [Gyr], [m(i), i = 1, n_filt], A_V, Ly forest
```

 and `OUTPUT_FILE.cat`, the random catalogue obtained from the `MODEL_CAT_FILE` adding a random noise. This is the simulated catalogue that can be used as photometric catalogue for **hyperz**. Its format will be:


```
id, [m(i), i = 1, n_filt], [Δm(i), i = 1, n_filt]
```
- **REF_FILTER**: the number of the filter (to be checked in the `filters.log` file) that will have a magnitude in the range between **MAG_MIN** and **MAG_MAX**.
- **MAG_MIN** and **MAG_MAX**: the magnitudes defining the range of apparent magnitudes attributed to the **REF_FILTER**.
- **NOISE_TYPE**: the type of noise adopted to compute the magnitudes in `NOISE_CAT_FILE` from `MODEL_CAT_FILE`: if **NOISE_TYPE** is 0, random noise with fixed sigma in magnitudes will be applied to magnitudes. Selecting 1, the noise Δm will be computed as a function of m following the approximation

$$\Delta m(m) \simeq \sqrt{\left[2.5 \log \left(1 + \frac{1}{S/N}\right)\right]^2 + \text{ERR_MAG_MIN}^2}, \quad (5)$$

where S/N is the signal to noise ratio, which is given as a function of the apparent magnitude through

$$S/N = (S/N)_0 10^{-0.4(m-m_0)}. \quad (6)$$

$(S/N)_0$ is the signal to noise ratio at a given reference magnitude m_0 . In the case **NOISE_TYPE** = 0, in the file `FILTERS_FILE` the column two must correspond to the sigma of the errors distribution; in the second case the columns two and three are the value of $(S/N)_0$ and m_0 respectively. If you chose the latter option, during the run of the program, the limiting magnitudes in each filter will be showed. We assume as limiting magnitudes the value at which the signal to noise ratio fall down 1. You can use these magnitudes in the `FILTERS_FILE` for **hyperz**. The magnitudes exceeding the limiting magnitudes will be set to 99.

- **N_OBJ**: the number of objects in the simulated catalogue.
- **Z_FORM**: the formation redshift of galaxies.
- **AGE_RANDOM**: the option for the galaxy ages computation. Setting the value 0 the age is assumed to be equal to the age of a galaxy at the redshift z chosen

column three the value of the transmission. Take care that if your response function contains more than 200 points, the program will proceed with a rebinning to include only 200 points, because otherwise the integration would be too CPU time consuming. Notice that the points must be ordered by increasing wavelengths. Moreover, do not care about the normalization of the transmission functions, because this operation will be performed internally in **hyperz**. In Figure 8 we illustrate the transmission functions of the most used filters, corresponding to the records # 12, 91, 92, 93, 94, 162, 76, 75, 77, 131, 122, 123, 124, 121.

Two reminder files are included in the package, even if they are not used during the computation: `./ZPHOT/filters/filters.log` contains the list of the filters contained in `./ZPHOT/filters/FILTER.RES`, their record number and the number of points composing their transmission function; `./ZPHOT/filters/filters.dat` contains a description of the filters by means of their λ_{eff} , their surface S , their width, computed as described in Section 3.2, and the conversion between Vega and AB magnitudes..

The program **hyperz** works with “standard” Vega magnitudes, as well as with AB magnitudes. The first photometric system is calibrated on the Vega Spectral Energy Distribution shown in Figure 9 and taken from the Bruzual & Charlot (1993) library. In the formulae we have

$$m_{\text{Vega}} = -2.5 \left[\log \int R(\lambda) f(\lambda) d\lambda - \log \int R(\lambda) f_{\text{Vega}}(\lambda) d\lambda \right],$$

where $f(\lambda)$ is in unit of $\text{erg s}^{-1} \text{cm}^{-2} \text{\AA}^{-1}$. AB magnitudes are defined in such a way that the zero point is set equal for all filters and are directly related to the flux $f(\nu)$: $m_{\text{AB}} = -2.5 \log f(\nu) - 48.60$, where $f(\nu)$ is given in $\text{erg s}^{-1} \text{cm}^{-2} \text{Hz}^{-1}$, and thus AB magnitudes can be monochromatic. An object having a flat spectrum will have equal magnitudes in all the filters. The conversion between Vega and AB magnitudes for a given filter is computed using the equation:

$$\text{conv}_{\text{AB}} = m_{\text{AB}} - m_{\text{Vega}} = m_{\text{AB}}(\text{Vega}) = -2.5 \log \frac{\int R(\nu) f_{\text{Vega}}(\nu) d\nu}{\int R(\nu) d\nu} - 48.60.$$

B FAQ

Q: The program compiles correctly, but when I execute it I obtain the following error message (or something like this):

```
Reading parameter file :
There are 5 synthetic spectra
open: No such file or directory
apparent state: unit 81 named ~/ZPHOT/filters/FILTER.RES
```

```
last format: list io
```

```
lately writing sequential formatted external IO
```

```
Abort (core dumped)
```

A: You are probably working with Linux, isn't it? In this OS the `~/` is not recognized as home directory, you have to write the whole path of files in the parameter files `hyperz.param` and `spectra.param`.

Q: I have the photometry measured in 3 filters. Can I compute photometric redshifts?

A: There are no technical problems running **hyperz** with only 3 filters, but the results will be not very reliable. If you look at the probability functions probably you will find multiple solutions and extended "plateaux".

Q: Do I need near-IR or UV to compute photometric redshifts?

A: No, you don't need specifically near-IR or UV. But then the accuracy in several redshift zones, especially at $z > 1$, is going to be severely decreased. You can check Bolzonella et al. (2000) for a complete study.

Q: Do I need to have the photometry in all the filters for each object?

A: If your object was in the field but not detected, then you have to set its magnitude $m > 90$ and choose between the different options that **hyperz** provides to deal with such case. If your object was not in the field, then set its magnitude $m < 1$ and **hyperz** will not consider it in the computation.

Q: Do I need to cite you if I write a paper using this code?

A: It will be greatly appreciated to include a note saying that your results were obtained using the publicly available software **hyperz**, to refer to the paper Bolzonella M., Miralles J.-M. & Pelló R. (2000) and to include the http address where you downloaded it.

Q: I have an unsolvable problem, who can I contact?

A: You can contact either Micol at `micol@ifctr.mi.cnr.it`, Roser at `roser@ast.obs-mip.fr` or Joan-Marc at `miralles@astro.uni-bonn.de`.

Q: When are you going to release a new version?

A: If you want to be informed of new releases, bug fixes or improvements, just email to any of us.

C Most important changes

Here we summarize the most important changes introduced in the version 1.2, for convenience of the users of the previous version.

1. parameter file
2. Lyman forest
3. absolute magnitude, AB in make_catalog
4. fixed bugs

D Important remarks

small differences between results obtained on different machines... double precision.

References

- [1] Allen C. W., 1976, in “Astrophysical Quantities”, University of London eds., The Athlone Press, pag. 264
- [2] Avni Y., 1976, ApJ 210, 642
- [3] Benítez N., 2000, ApJ 536, 571
- [4] Bertin E. & Arnouts S., 1996, A&AS 117, 393
- [5] Bolzonella M., Miralles J.-M. & Pelló R., 2000, A&A 363, 476
- [6] Bouchet P., Lequeux J., Maurice E., Prévot L. & Prévot-Burnichon M. L., 1985, A&A 149, 330
- [7] Brunner R. J., Connolly A. J., Szalay A. S. & Bershadsky M. A., 1997, ApJL 482, L21
- [8] Bruzual G. & Charlot S., 1993, ApJ 405, 538
- [9] Calzetti D., Armus L., Bohlin R. C., Kinney A. L., Koornneef J. & Storchi-Bergmann T., 2000, ApJ 533, 682
- [10] Coleman G. D., Wu C. C., Weedman D. W., 1980, ApJS 43, 393
- [11] Connolly A. J., Csabai I., Szalay A. S., Koo D. C., Kron R. G. & Munn J. A., 1995, AJ 110, 2655
- [12] Fernández-Soto A., Lanzetta K. M. & Yahil A., 1999, ApJ 513, 34
- [13] Fitzpatrick E. L., 1986, AJ 92, 1068
- [14] Fukugita M., Shimasaku K. & Ichikawa T., 1995, PASP 107, 945
- [15] Lanzetta K. M., Yahil A. & Fernández-Soto A., 1996, Nature 381, 759
- [16] Madau P., 1995, ApJ 441, 18
- [17] Miller G. E. & Scalo J. M., 1979, ApJS 41, 513
- [18] Miralles J.-M., 1998, PhD thesis, Université Paul Sabatier, Toulouse
- [19] Oke J. B. & Korycansky D. G., 1982, ApJ 255, 11
- [20] Pelló R., Miralles J.-M., Le Borgne J.-F., Picat J.-P., Soucail G. & Bruzual G., 1996, A&A 314, 73
- [21] Prévot M. L., Lequeux J., Prévot L., Maurice E. & Rocca-Volmerange B., 1984, A&A 132, 389
- [22] Salpeter E. E., 1955, ApJ 121, 161
- [23] Scalo J. M., 1986, Fundam. Cosmic Phys. 11, 1
- [24] Schmidt M., 1959, ApJ 129, 243
- [25] Seaton M. J., 1979, MNRAS 187, 73
- [26] Tinsley B. M., 1980, Fundam. Cosmic Phys. 5, 287

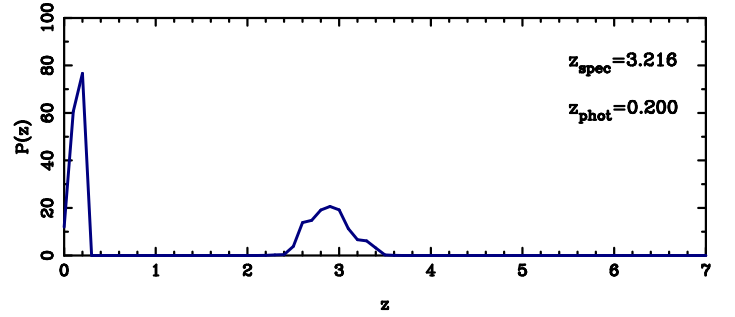
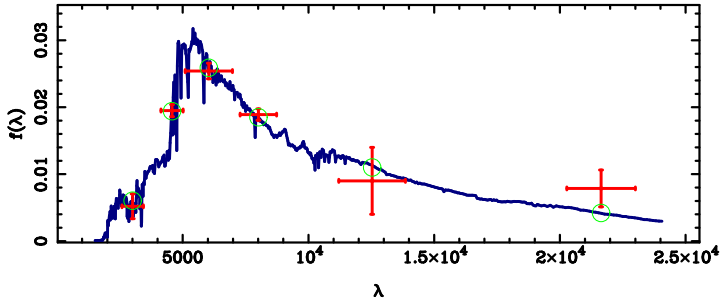
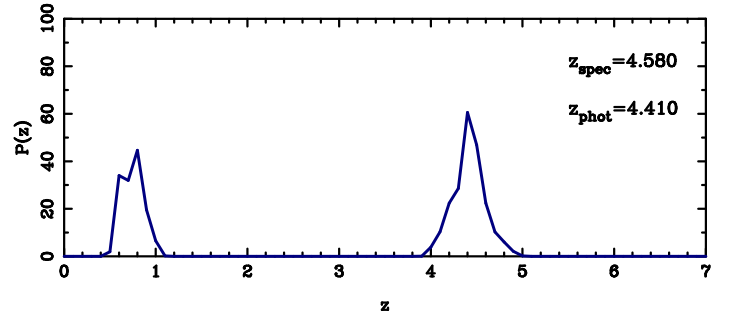
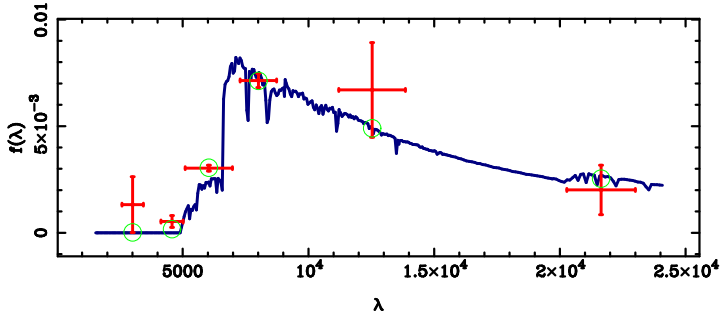
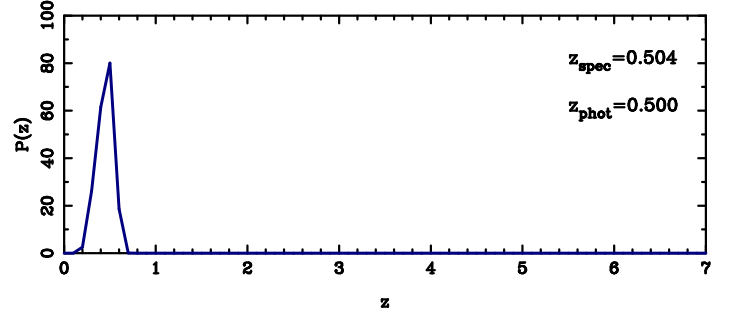
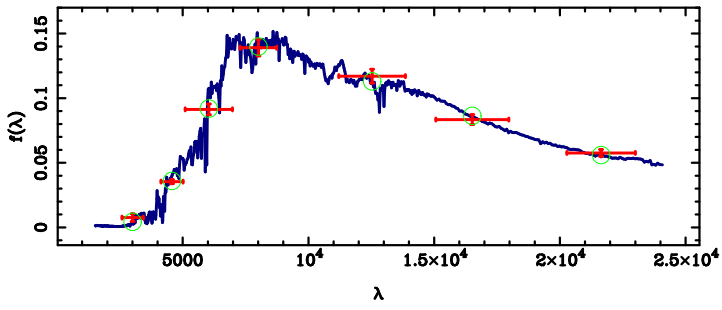


Figure 7: *Left*: The best fit SED (solid line), with superimposed the observed points with error bars (vertical error bars correspond to photometric errors, horizontal error bars represent the surface covered by the filter) and the fluxes derived from the best fit SED (circles). *Right*: The probability functions relative to χ^2 for the three considered objects.

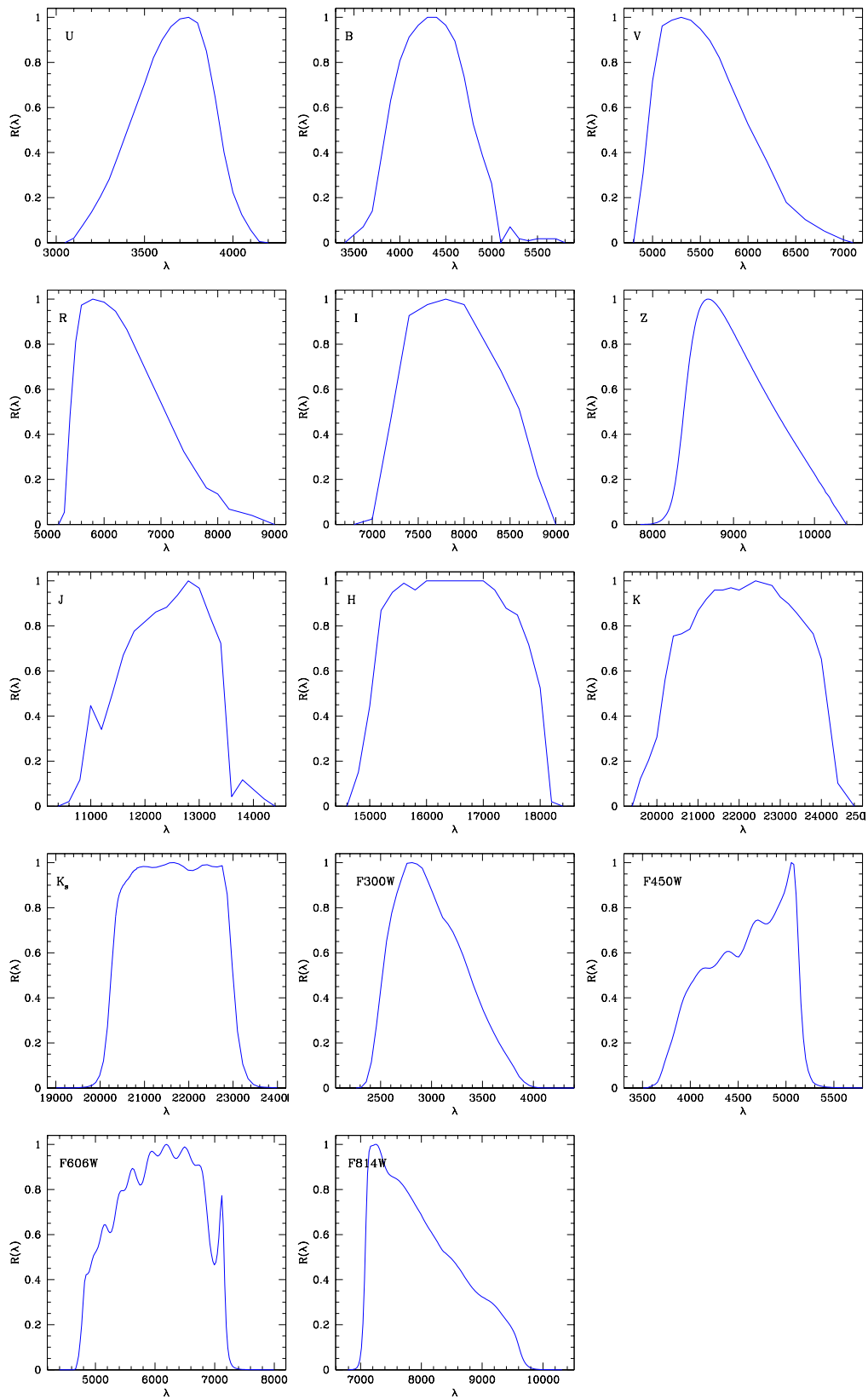


Figure 8: Normalized filter's transmission functions of some of the most used filters.

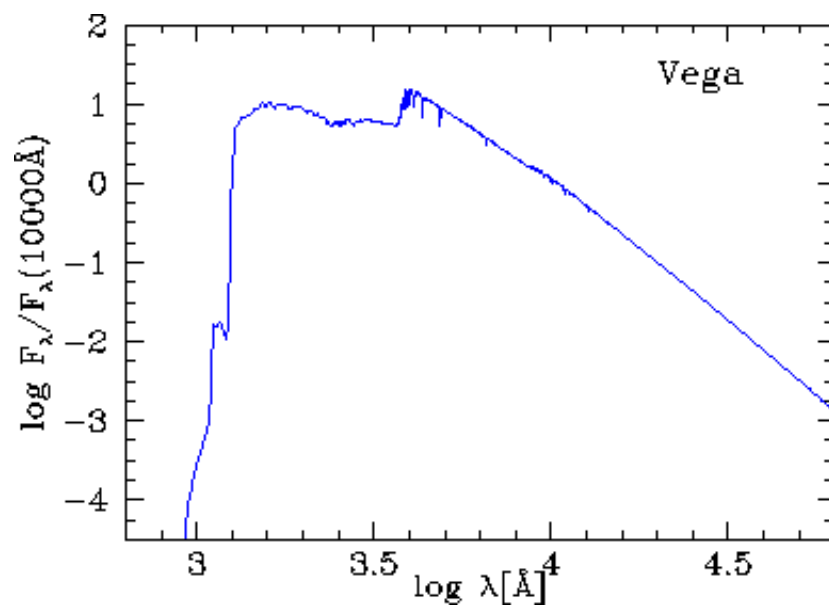


Figure 9: Spectral Energy Distribution of α Lyrae (Vega). Data from GISSEL library.